PLOS ONE

RESEARCH ARTICLE

# Functional Brain Dysfunction in Patients with Benign Childhood Epilepsy as Revealed by Graph Theory

**Azeez Adebimpe[1], Ardalan Aarabi[1]*, Emilie Bourel-Ponchel[1,2], Mahdi Mahmoudzadeh[1,2], Fabrice Wallois[1,2]**

**1** Institut National de la Santé et de la Recherche Médicale (INSERM U1105), Centre Universitaire de Recheche en Santé (CURS), University Hospital, Amiens, France, **2** Explorations Fonctionnelles du Système Nerveux (EFSN) pédiatrique, University Hospital, Amiens, France

* ardalan.aarabi@u-picardie.fr





**Citation:** Adebimpe A, Aarabi A, Bourel-Ponchel E, Mahmoudzadeh M, Wallois F (2015) Functional Brain Dysfunction in Patients with Benign Childhood Epilepsy as Revealed by Graph Theory. PLoS ONE 10(10): e0139228. doi:10.1371/journal.pone.0139228

**Editor:** Bin He, University of Minnesota, UNITED STATES

**Received:** June 8, 2015

**Accepted:** September 10, 2015

**Published:** October 2, 2015



**Data Availability Statement:** Patient data (EEG recordings) used for this publication contain confidential information and therefore cannot be shared. Essential analysis subroutines written in Matlab can be obtained from the first authors on request, ardalan.aarabi@u-picardie.fr.

**Funding:** The fund is from INSERM (Institut national de la santé et de la recherche médicale, www.inserm.fr). The funders had no role in study design, data collection and analysis, decision to publish, or preparation of the manuscript.

## Abstract

There is growing evidence that brain networks are altered in epileptic subjects. In this study, we investigated the functional connectivity and brain network properties of benign childhood epilepsy with centrotemporal spikes using graph theory. Benign childhood epilepsy with centrotemporal spikes is the most common form of idiopathic epilepsy in young children under the age of 16 years. High-density EEG data were recorded from patients and controls in resting state with eyes closed. Data were preprocessed and spike and spike-free segments were selected for analysis. Phase locking value was calculated for all paired combinations of channels and for five frequency bands (δ, θ, α, $\beta_1$ and $\beta_2$). We computed the degree and small-world parameters—clustering coefficient (C) and path length (L)—and compared the two patient conditions to controls. A higher degree at epileptic zones during interictal epileptic spikes (IES) was observed in all frequency bands. Both patient conditions reduced connection at the occipital and right frontal regions close to the epileptic zone in the α band. The "small-world" features (high C and short L) were deviated in patients compared to controls. A changed from an ordered network in the δ band to a more randomly organized network in the α band was observed in patients compared to healthy controls. These findings show that the benign epileptic brain network is disrupted not only at the epileptic zone, but also in other brain regions especially frontal regions.

## Introduction

Benign childhood epilepsy with centrotemporal spikes (BCECTS) is the most common childhood epilepsy syndrome, usually affecting the children under the age of 16 years [1,2]. Several studies have demonstrated different cognitive impairments [3] including frontal dysfunction [4] in patients with benign epilepsy with no evidence of large structural changes compared to other forms of epilepsy [5,6]. However, all forms of epilepsy are associated with abnormal brain activity and impaired neural processing as a result of unstable brain dynamics and

**Competing Interests:** The authors have declared that no competing interests exist.

networks [7]. Dynamic changes of epileptic brain networks are believed to be caused by dysregulation of neurotransmitters leading to abnormal electrical activity [8].

Abnormal synchronization of neurons, probably due to changes in the spatial organization of the neural networks, is also thought to contribute to the generation and propagation of epileptic seizures [9]. Graph theory is a promising mathematical approach to study topological characteristics of both local and long distance brain functional connectivity using fMRI, EEG and MEG [10–12]. Graph analysis of brain connectivity has revealed reconfiguration of both structural and functional connections between different neural networks in several brain disorders [13]. Few studies have compared the resting state of healthy controls to that of epileptic patients at network level [14]. The characterization of the dynamics of the cortical networks in scalp EEG and electrocorticography (ECoG) in epileptic patients during the resting state has demonstrated disruptions in global and regional brain networks [15–17].

A large number of graph metrics have been proposed, two of which, clustering coefficient and path length [18], have been mostly used to characterize the functional connectivity of human brain networks [13,19]. The clustering coefficient (C) is a measure of functional segregation quantifying the presence of locally connected groups known as clusters or modules, which indicate segregated neural processing [18]. Path length (L), however, measures network integration by estimating the effective communications between different brain regions [18]. A graph comprising numerous local and few long-distance connections (high C and short L) most closely corresponds to the optimal network, called the 'small-world network (SWN)', which is intermediate between ordered (high C and long L) and random networks (low C and short L) [20,21]. However, various types of neurological diseases, including epilepsy, have been reported to deviate from SWN properties [22–24].

In this study, we investigated changes in brain functional connectivity in BCECTS patients compared to healthy controls in various frequency bands using high-density resting EEG data under the eyes-closed condition. For this purpose, we quantified the topological properties of the BCECTS brain networks at rest during periods with and without interictal epileptic spikes (IES) by estimating the clustering coefficient (C) and path length (L) from the functional connectivity matrices reconstructed with phase locking value (PLV). We also estimated the degree of centrality that measures the number of connections between a particular node (a specific brain region) to other nodes [18]. In summary, this study was designed to investigate whether BCECTS functional brain networks in the presence or absence of interictal spikes exhibited characteristic changes in small-world network features.

## Materials and Methods

### Subjects

Our study was conducted at Amiens University Hospital (Amiens, France) and approved by the hospital's ethics committee (CPP Nord-Ouest 2, approval No. 2011-A00782-39). Written consent approved by the ethics committee was obtained from parents/caregivers. Eight healthy adolescents (9 ± 0.21 years old) and nine young patients (9 ± 0.24 years old) with BCECTS were included in this study. All patients presented right centrotemporal spikes (see S1 Fig) and were free of any other neurological disorder at the time of the study.

### EEG recording and preprocessing

On average, thirteen-minute high-resolution EEG data were recorded from each subject resting comfortably in a supine position in a quiet room. EEG data were recorded with 64 channels based on the international 10–10 system and a sampling rate of 256 Hz. An average reference montage was used for all of the analysis. Data were filtered offline between 0.5 to 30 Hz to

exclude high-frequency noise including muscle activities. To identify EEG portions with ocular and movement artifacts, which were excluded from the analysis, the EEG recordings were first normalized by the Z-score transformation and then processed semi-automatically (with visual inspection) using a simple threshold method (threshold set to the mean of the z-score distribution for each channel) as it was implemented in Fieldtrip software (http://www.fieldtriptoolbox.org/tutorial/visual_artifact_rejection) [25]. Two neurophysiologists visually inspected the filtered data in order to identify spikes segment and artifacts.

Artifact-free portions of the EEG data were partitioned into two-second non-overlapping segments. Five segments were randomly selected for each of the control subjects (CON). Two conditions were defined for the epileptic group: 5 segments with interictal spikes (With Spike Condition—WSC) and 5 spike-free segments (No Spike Condition—NSC), all randomly selected. On average, the WSC EEG segments contained 7 spikes considered as a requirement to ensure homogeneity across the patients.

## Functional Connectivity

Pairwise correlations between all EEG channels were computed with the Phase Locking Value (PLV) [26,27]. Briefly, the PLV belongs to the family of phase synchronization values that are used to estimate functional connectivity between two signals based on their relative phase differences. To calculate the PLV, we first filtered the data into frequency bands (δ (0.5–3.5 Hz), θ (4–8 Hz), α (8.5–13 Hz), $\beta_1$ (13.5–20 Hz) and $\beta_2$ (20.5–30 Hz) using zero-phase forward and reverse digital filtering. The analytical signals were obtained by Hilbert transformation of the filtered signals. The Hilbert transformed signals consisted of the instantaneous amplitude and phase of the signals. The phase angle (φ) was used to compute the PLV. The PLV ranged from 0 to 1, with 0 and 1 indicating no connection and maximum connection between any given pair of signals, respectively. The end-result of computing the PLV for all paired combinations of channels was a square matrix of size 63 (number of EEG channels), in which each entry $N_{x,y}$ (= $N_{y,x}$) contained the PLV for channels x and y (see Supporting information for more details).

## Computation of graph theory parameters

A graph is a basic topographical representation of a network consisting of nodes or vertices (in this case brain regions or electrodes) and edges (correlation between nodes). In this study, the network consisted of 63 vertices (electrodes) connected by edge weights (or elements) between all pairs of channels. The first step in applying graph theoretical analysis to functional connectivity matrices consists of converting the matrix into a binary graph, in which the edges either exist (1) or do not exist (0), i.e, with no graded values. Functional connectivity matrices were converted to binary graphs by applying an optimal threshold, τ above/below which connectivity values were set to 1/0. This operation transformed functional connectivity matrices to binary adjacency matrices, which was then followed by computation of graph metrics.

For each subject and frequency band, we determined the optimal threshold using an iterative method to make sure that the proportion and global spatial distribution of connections between brain regions were similar across subjects. We did not, however, choose a single threshold for all frequency bands mainly because it could lead to false positives in some frequency bands resulted from highly disconnected or over-densely networks [28]. Our threshold optimization procedure was based on the computation of the degree, which is defined for each node as the number of links connected to the node. The degree is used to measure the importance of individual nodes (nodes with a high degree of interaction with other nodes). The optimal thresholds were iteratively determined by means of the following procedure. First, for each functional connectivity matrix, we set the threshold to one standard deviation above the

median connectivity value. We then calculated the mean degree for the whole brain network. The optimal threshold was determined under two conditions, (i) the mean degree must not be less than 2ln(N), and (ii) at least 95% of nodes must be connected to one or more nodes [28,29] (see SI for more information). These conditions were then used to optimize the connection strength, which was used to increase the signal-to-noise ratio and to reduce false-positive edges in the graph [29].

To investigate the global topology of large-scale brain functional networks in patients and controls, the optimal threshold for each subject and frequency band was applied to the functional connectivity matrix for computation of degree of the whole brain network. We then investigated whether the occurrence of interictal spikes could change the small-world network features (C and L) in BCECTS brain networks. The clustering coefficient of a node is the ratio of the number of actual edges to the total number of potential edges adjacent to the node. The clustering coefficient was computed for all nodes and averaged (mean clustering coefficient, C). The path length is the mean shortest path connecting any two nodes of the graph and indicates how well the nodes are interconnected or integrated [18,20]. Similarly, we computed the mean path length (L) of the whole brain network (see SI for mathematical description). C and L were computed as a function of network density defined as the ratio of the actual number of edges in the graph to the total number of possible edges. In order to detect significant differences in network organization between the groups and to minimize the number of false (or noisy) edges in the networks, we only investigated strong connections by changing the network density from 30% to 60% in steps of 5% based on previous studies [30,31].

## Statistical analysis

Nonparametric permutation testing was used for all graph parameters with correction for multiple comparisons including *post hoc* tests with a p-value $\leq 0.05$. A total of 1,000 permutations were used to determine the significance level for each test [32]

All computations and statistical analyses were performed in Matlab with custom scripts and open source toolboxes: Fieldtrip (http://fieldtrip.fcdonders.nl/), EEGLAB (for 3D topological plots, http://sccn.ucsd.edu/eeglab/), and the brain connectivity toolbox (for graph parameter computations, https://sites.google.com/site/bctnet/).

# Results

## Synchronization and degree

The mean PLV was analysed under the three conditions in order to investigate differences in synchronization between patients and controls (Fig 1). As shown, the mean PLV under the with-spike condition exhibited significantly higher values in the θ band compared to the other two conditions (CON and NSC). No significant differences in synchronization were observed between the groups in the other frequency bands.

Compared to controls, BCECTS patients were characterized by significantly lower mean degree values in the δ band (under both WSC and NSC) and in the $\beta_1$ band (only under NSC).

We also investigated whether our results were affected by the precise choice of the thresholds. As shown in Table 1, within each group the variations in PLV and K due to changes in the optimal thresholds were very small for each particular frequency band.

We further investigated the regional differences in the degree (K) distribution between the groups (Fig 2). In the presence of IES (WSC vs. CON), K significantly increased in the right centrotemporal region (IES generator region), and decreased in the occipital region in almost all frequency bands. Right frontocentral areas exhibited lower K values in mid-range

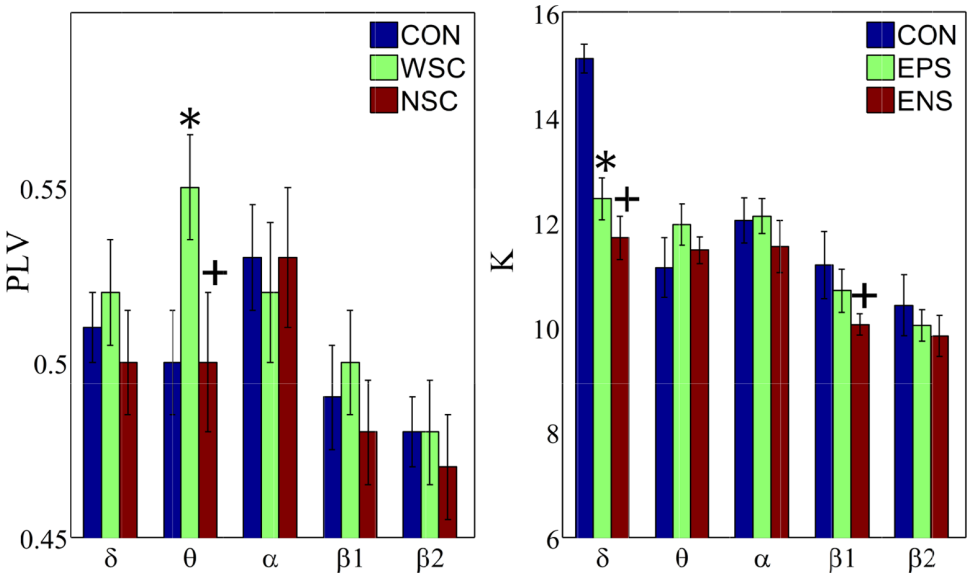


**Fig 1. Group mean Phase Locking Value (PLV) and group mean degree (K).** Error bars show standard errors with 95% confidence intervals. CON, WSC and NSC indicate the control, with spike and no spike conditions, respectively. Statistical significance is denoted by * (WSC vs CON) and + (NSC vs CON) with $p<0.05$.

doi:10.1371/journal.pone.0139228.g001

frequencies (θ and α). On the contralateral side, however, the degree significantly increased in the left frontal and frontotemporal regions in the θ band.

In the absence of IES (NSC vs. CON), K increased in the left frontal region in the θ band and in right centrotemporal areas in high frequencies ($\beta_1$ and $\beta_2$). In the mid- and high-range frequencies, patients exhibited relatively lower values of degree in occipital areas.

Compared to NSC, WSC was characterized with significant increases of K in the right centrotemporal regions in the δ and α band, and in the right parietotemporal regions in the $\beta_1$

**Table 1. Mean and range of changes (at 95% confidence interval) of phase locking value (PLV), threshold ($\tau$) and degree (K) computed for each group and frequency band.**

| | Frequency band | PLV | τ | K |
|---|---|---|---|---|
| **CON** | δ | 0.51±0.02 | 0.59±0.01 | 15.12±1.40 |
| | θ | 0.50±0.03 | 0.60±0.01 | 11.14±1.13 |
| | α | 0.53±0.03 | 0.63±0.02 | 12.04±0.86 |
| | $\beta_1$ | 0.49±0.03 | 0.57±0.01 | 11.19±1.28 |
| | $\beta_2$ | 0.48±0.02 | 0.54±0.01 | 10.42±1.16 |
| **WSC** | δ | 0.52±0.03 | 0.63±0.02 | 12.45±0.80 |
| | θ | 0.55±0.03 | 0.64±0.01 | 11.96±0.79 |
| | α | 0.52±0.04 | 0.62±0.03 | 12.12±0.66 |
| | $\beta_1$ | 0.50±0.03 | 0.58±0.01 | 10.70±0.81 |
| | $\beta_2$ | 0.48±0.03 | 0.55±0.00 | 10.04±0.59 |
| **NSC** | δ | 0.50±0.03 | 0.60±0.03 | 11.71±0.82 |
| | θ | 0.50±0.04 | 0.60±0.02 | 11.47±0.50 |
| | α | 0.53±0.04 | 0.62±0.04 | 11.54±1.00 |
| | $\beta_1$ | 0.48±0.03 | 0.55±0.01 | 10.06±0.41 |
| | $\beta_2$ | 0.47±0.03 | 0.53±0.01 | 9.83±0.79 |

doi:10.1371/journal.pone.0139228.t001

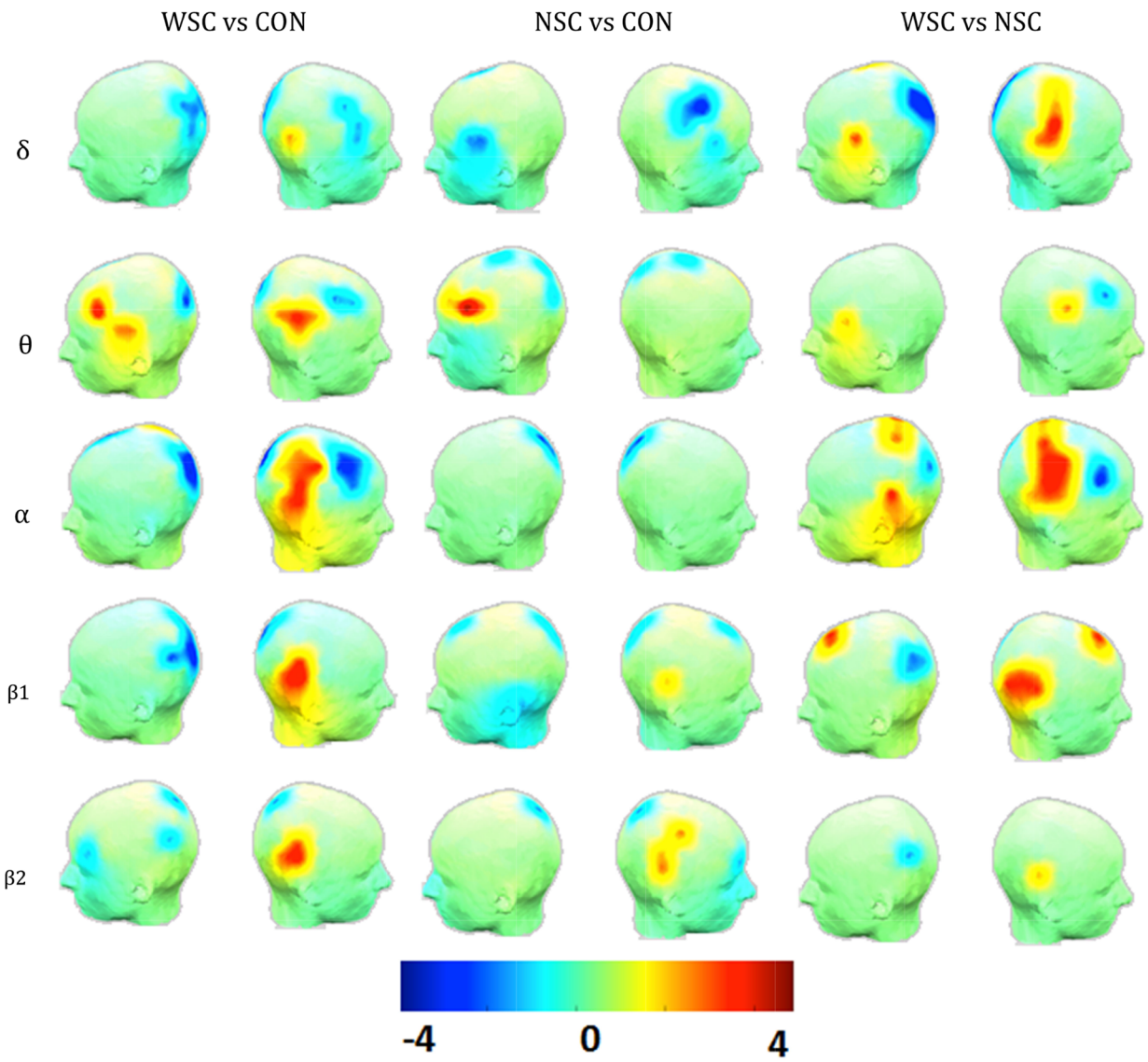


**Fig 2. Statistical difference (t-value) maps of degree between the control (CON) and the epileptic groups (WSC and NSC).** The color bar indicates the t values projected onto a standardized head shape. The significant increase (indicated by red) and decrease (indicated by blue) in degree have been represented, respectively, by positive and negative t values resulted from statistical comparisons between (WSC and CON), (NSC and CON), and (WSC and NSC).

doi:10.1371/journal.pone.0139228.g002

band. The degree decreased significantly in occipital areas in all frequencies except in the θ band, in the right frontocentral region close to the spike generation zone in mid-range frequencies (θ and α), and in the left posterior region in the $\beta_1$ band.

## Clustering coefficient and path length

Fig 3 shows the mean clustering coefficient (C) and mean path length (L) computed for each condition.

In low frequencies (δ), the presence of IES (WSC) in the EEG segments significantly increased C at low connection densities (<50%) in comparison to the other two conditions.

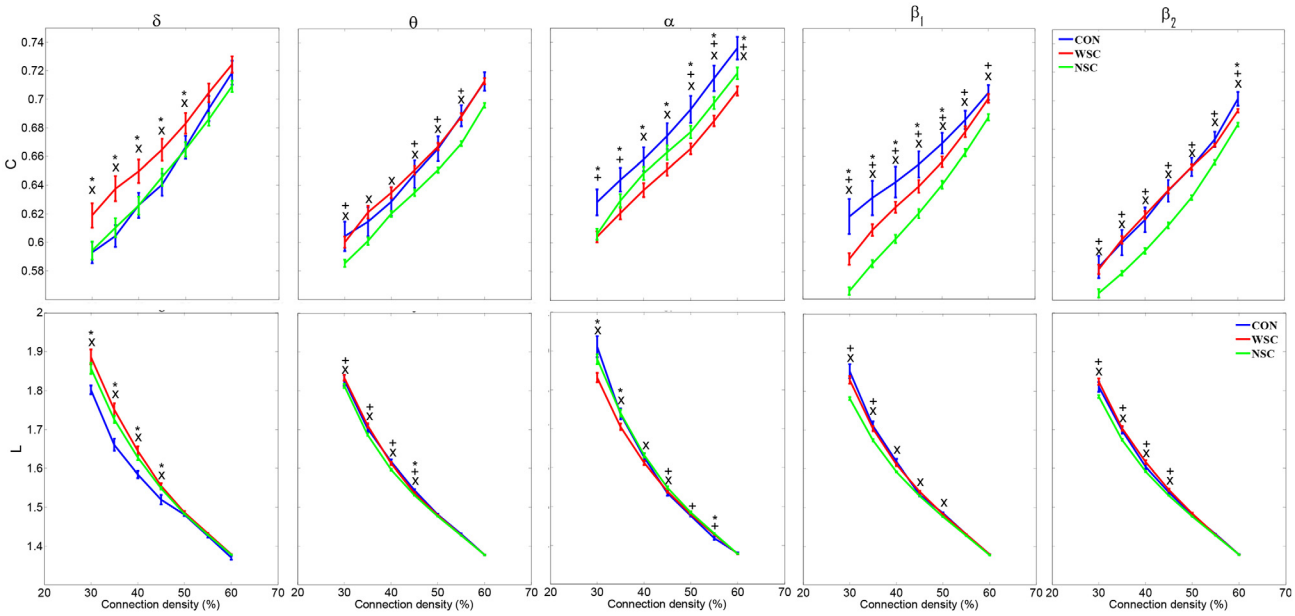


**Fig 3. Mean clustering coefficient (C) and mean path length (L) as a function of network density for each frequency band.** The error bars represent standard error with 95% confidence intervals. CON, WSC and NSC indicate the control, with spike and no spike conditions, respectively. Statistical significance is denoted by * (WSC vs. CON), + (NSC vs. CON) and × (WSC vs. NSC) with $p<0.05$.

doi:10.1371/journal.pone.0139228.g003

Compared to CON, both epileptic conditions exhibited shorter path length at connection densities up to 45%.

In the θ band, compared to NSC, WSC and CON showed significantly higher C (for all connection densities) and longer L (for connection densities less than 40%). No significant differences in clustering coefficients were observed between WSC and CON at almost all connection densities.

In the α band, both NSC and WSC compared to CON, and WSC compared to NSC exhibited significantly lower C values for almost all connection densities. Similar differences in L were found between the groups on a less significant level. The only exception was shorter path lengths found for WSC compared to CON and NSC at connection densities up to 45%.

In higher frequencies ($\beta_1$ and $\beta_2$), lower C (over all connection densities) and shorter L (for connection densities less than 45%) were found under NSC (vs. WSC and CON). In the $\beta_1$ band, compared to CON, WSC was characterized by significantly lower clustering coefficients. Table 2 roughly summarizes overall significant differences between the conditions.

**Table 2. Summary of differences in mean clustering coefficient (C) and mean path length (L) between the three conditions as shown in Fig 3.**

| | C | | | | | L | | | | |
|---|---|---|---|---|---|---|---|---|---|---|
| | **δ** | **θ** | **α** | **$\beta_1$** | **$\beta_2$** | **δ** | **θ** | **α** | **$\beta_1$** | **$\beta_2$** |
| **WSC vs. NSC** | ↑ | ↑ | ↓ | ↑ | ↑ | NS | ↑ | ↓ | ↑ | ↑ |
| **WSC vs. CON** | ↑ | NS | ↓ | ↓ | NS | ↑ | NS | ↓ | NS | NS |
| **NSC vs. CON** | NS | ↓ | ↓ | ↓ | ↓ | ↑ | ↓ | ↓ | ↓ | ↓ |

↑ and ↓ indicate significant increase and decrease in C and L between conditions, respectively. NS represents non-significant differences.

doi:10.1371/journal.pone.0139228.t002

## Discussion

This study investigated differences in the brain functional connectivity between BCECTS patients and healthy controls. Statistical dependencies between EEG time-series recorded from different brain regions were investigated by computing functional interactions using PLV as a measure of phase synchronization as well as graph metrics. The brain functional connectivity of BCECTS patients was found to be disrupted in terms of synchronization and degree of connectivity not only in the IES zone but also in frontal and temporal areas. Deviations from small-world features and network parameters were also observed in various frequency bands in BCECTS patients regardless of the presence or absence of spikes in EEG segments.

Many studies have shown that neurological diseases in children [33,34] are associated with differences in the level of synchronization compared to healthy controls. Compared to the other frequency bands, we found higher synchronization values in the α band in healthy subjects (Fig 1). The increased α synchronization is generally accepted to be due to the increased alpha activation under the eyes-closed resting state of the brain [35]. However, compared to controls, BCECTS patients exhibited significantly increased θ and decreased α synchronization under the with-spike condition. Our observations are consistent with those reported in patients with temporal lobe epilepsy [30], who presented significantly increased synchronization in the θ band, but non-significantly decreased synchronization in the α band. The increase of θ synchronization is commonly observed, not only in epilepsy [36,37] but also in other neurological diseases such as Parkinson's disease [38] and Alzheimer's disease [39].

### Interictal spikes disrupt the global topology of brain functional connectivity

The disruption of brain dynamics in BCECTS patients probably results in higher levels of synchronization in some regions of the brain (especially in the epileptogenic zone) and lower levels of synchronization in other regions due to epileptic spikes. Although there is little evidence to suggest that BCECTS is associated with structural brain abnormalities [40], we found strong frequency-dependent changes in the degree as a measure of centrality or information coordination implying disrupted functional connectivity in the epileptic zone in BCECTS patients.

However, increased and decreased degrees in other regions, notably frontal and occipital, support the idea that disruption of brain functional connectivity in BCECTS patients is unlikely to be restricted to the epileptogenic zone. This finding may reflect the functional reorganization of the BCECTS brain network topology.

### Functional disruption of BCECTS frontal networks

Our results revealed functional dysfunction of frontal brain networks in the presence/absence of interictal epileptic spikes. Compared to controls, BCECTS patients were characterized by a reduced degree in the right frontal region in the α band and an increased degree in the left frontal region in the θ band. These observations suggest functional network reorganization in the frontal regions regardless of the presence or absence of spikes in EEG segments. This frontal functional dysfunction may confirm the results of longitudinal MRI studies [41], which suggested that learning and memory difficulties in BCECTS patients may be associated with serial changes in the frontal and prefrontal lobes [42–44].

The alteration of brain functional connectivity in the absence of IES does not exclusively affect the frontal regions; it also involves the occipital region. This spatial pattern of changes

was also observed in the presence of IES, especially in the α band. The decreased degree in the α band in the posterior region under the epileptic conditions may support the disruption of functional brain connectivity in BCECTS patients even though the differences in global synchronization did not reach statistical significance. Since in healthy controls the functional connectivity has been shown to increase in frontal and posterior regions under the eyes-closed condition in the α band [45], in BCECTS patients the reduced α degree at the occipital region may support their poor visual spatial memory [46].

## Deviation from small-world network features

There has been a growing interest in small-world analysis of brain networks in various neurological diseases [13]. The small-world network features of healthy controls have been compared to different brain diseases, such as schizophrenia [47], depression [48], Alzheimer's disease [24] and various types of epilepsy [14]. Most of these neurological diseases are associated with lower clustering coefficients and shorter path lengths compared to healthy controls.

The present study demonstrated frequency-dependent alterations of small-world features and network parameters in BCECTS patients in the presence and in the absence of IES. In the δ band, patients under the WSC condition exhibited higher C and long L compared to controls, implying that, at very low frequencies, BCECTS brain networks exhibit more functionally ordered organization in the presence of IES. This observation is consistent with the findings observed in other types of epilepsy [49]. In higher frequency bands (α and $\beta_1$), patients showed lower C values under both WSC and NSC compared to controls. The simultaneous decrease in C and L in the $\beta_1$ band may indicate loss of global processing and stronger integration between long-distance brain regions, which can be interpreted as increased functional interaction between long-range brain connections in BCECTS patients.

Interestingly, a switch in the brain network functional organization in the θ and α bands was observed when comparing WSC and NSC conditions. BCECTS patients' brain networks tended to change from a more randomly organized network (low C, short L) in the α band to a functionally ordered network (high C, long L) in the θ and β bands due to IES. The global increase in C in the presence of IES (excluding the α band) reflects orderly connection of IES brain networks. This finding is in agreement with studies on the other types of epilepsies using intracranial EEG and ECoG [16,50]. Small-world networks allow more rapid information processing and learning than either random or regular networks [51] and the results may suggest that the cognitive impairments observed in BCECTS may be associated with rapid changes in the functional reconfiguration of BCECTS brain networks. Although the shorter path length in higher frequency bands (in the α band for WSC and the β band for NSC has been shown to support effective interactions between and across brain regions [21], BCECTS brain networks may more closely resemble randomly organized networks.

In the absence of IES, C was lower in all frequency bands and L was lower in the θ and β bands in BCECTS patients compared to controls, indicating that, in the absence of IES, the BCECTS brain network is less ordered regardless of the frequency band except for the α band. It is generally believed that random networks ensure even better synchronization than small-world networks [52], as pathological random networks present rapid phase transition that could lead to the onset of interictal epileptic discharges. In agreement with our observations, temporal lobe epilepsy [30] has been characterized by lower C and shorter L in the α band compared to controls. These discrepancies between TLE and BCECTS are clinically relevant and may constitute a specific biomarker of the type of epilepsy. However, to confirm our findings, further study with a larger population of patients will be needed.

## Limitations and future directions

A potential limitation of our study is the use of scalp EEG for the functional connectivity analysis. In studies on epilepsy, scalp EEG is usually used for EEG source imaging and/or functional connectivity analysis [53], are employed for localizing the epileptogenic foci and investigating the functional organization of the epileptic cortical networks, respectively. In our study, we used PLV as a measure of undirected functional connectivity between electrodes to explore the global topology and dynamics of the interactions between large-scale brain regions during the interictal state over a range of frequencies. The functional connectivity analysis in the sensor space might provide inaccurate information on the overall organization of the cortical region mainly because EEG electrodes detect spatially averaged overlapping EEG signals from several brain sources or the signal generated by a focal cerebral source can be detected by nearby electrodes [54].

Our main direction of future work will be to use the EEG source space connectivity tools such as the directed transfer function (DTF)[55] or the Phase-Slope Index (PSI) [56] for the identification and characterization of the cortical networks involved in the interictal states.

In patients with epilepsy, the functional connectivity analysis using DTF has provided promising results using scalp EEG [57] and ECoG [58] for exploring the directed functional connectivity between cortical regions and the propagation of activation [58,59]. In general, the EEG functional connectivity analysis between neighbouring voxels might lead to spurious and over-represented results [60] because of the volume conduction effect which highly affects the accuracy of the functional connectivity tools [61]. However, DTF has been shown to be insensitive to volume conduction and less sensitive to noise [62]. We will also increase the number of electrodes to improve the accuracy of the functional connectivity analysis in the source space [63,64].

## Conclusion

This study investigated functional alterations in small-world characteristics in patients with benign epilepsy with centrotemporal spikes and showed that the functional organization of BCECTS brain networks changed from an ordered structure in low frequency bands (δ and θ bands) to a less randomly ordered network in higher frequency bands (α band).

This study provides further evidence that the BCECTS brain network is altered. The degree spatial distribution showed that alteration of the functional connectivity in the BCECTS brain was not limited to the epileptogenic zone, but also involved other regions, especially the frontal and occipital regions. The decreased connection density in the occipital and right frontal regions supports functional impairment of these regions. The BCECTS brain with IES, which does not present the features of a small-world network, showed topological characteristics of an ordered network in the δ band and a less ordered network in the α band. A more randomly organized network was also observed in the absence of IES compared to healthy controls.

## Supporting Information

**S1 Fig. Dipole locations of the averaged spikes for patients.**
(DOCX)

**S2 Fig. A sample interictal EEG recording from patient 1.** The spikes have been outlined in blue.
(DOCX)

**S3 Fig.** (A) Example of the functional connectivity matrix obtained for Subject 1. (B) The distribution of the PLV values of the functional connectivity matrix; the vertical line shows the

optimal threshold. (C) The binarized functional connectivity matrix obtained after applying the optimal threshold.
(DOCX)

**S1 Materials.**
(DOCX)

## Author Contributions

Conceived and designed the experiments: A. Adebimpe A. Aarabi EB MM FW. Performed the experiments: EB MM. Analyzed the data: A. Adebimpe A. Aarabi. Contributed reagents/materials/analysis tools: A. Adebimpe A. Aarabi EB MM FW. Wrote the paper: A. Adebimpe A. Aarabi FW. Read and accepted the manuscript: A. Adebimpe A. Aarabi EB MM FW.

## References


1. Shields WD, Snead OC. Benign epilepsy with centrotemporal spikes. Epilepsia. 2009; 50 Suppl 8: 10–15. doi: 10.1111/j.1528-1167.2009.02229.x PMID: 19702727
2. Camfield CS, Berg A, Stephani U, Wirrell EC. Transition issues for benign epilepsy with centrotemporal spikes, nonlesional focal epilepsy in otherwise normal children, childhood absence epilepsy, and juvenile myoclonic epilepsy. Epilepsia. 2014; 55 Suppl 3: 16–20. doi: 10.1111/epi.12706 PMID: 25209080
3. Datta AN, Oser N, Bauder F, Maier O, Martin F, Ramelli GP, et al. Cognitive impairment and cortical reorganization in children with benign epilepsy with centrotemporal spikes. Epilepsia. 2013; 54: 487–494. doi: 10.1111/epi.12067 PMID: 23297860
4. Kanemura H, Aihara M. Growth disturbance of frontal lobe in BCECTS presenting with frontal dysfunction. Brain Dev. 2009; 31: 771–774. doi: 10.1016/j.braindev.2008.12.007 PMID: 19168301
5. Coan AC, Campos BM, Yasuda CL, Kubota BY, Bergo FP, Guerreiro CA, et al. Frequent seizures are associated with a network of gray matter atrophy in temporal lobe epilepsy with or without hippocampal sclerosis. PloS One. 2014; 9: e85843. doi: 10.1371/journal.pone.0085843 PMID: 24475055
6. Huang W, Lu G, Zhang Z, Zhong Y, Wang Z, Yuan C, et al. Gray-matter volume reduction in the thalamus and frontal lobe in epileptic patients with generalized tonic-clonic seizures. J Neuroradiol J Neuroradiol. 2011; 38: 298–303. doi: 10.1016/j.neurad.2010.12.007 PMID: 21354624
7. Cressman JR, Ullah G, Ziburkus J, Schiff SJ, Barreto E. The influence of sodium and potassium dynamics on excitability, seizures, and the stability of persistent states: I. Single neuron dynamics. J Comput Neurosci. 2009; 26: 159–170. doi: 10.1007/s10827-008-0132-4 PMID: 19169801
8. Werner F-M, Coveñas R. Classical neurotransmitters and neuropeptides involved in generalized epilepsy: a focus on antiepileptic drugs. Curr Med Chem. 2011; 18: 4933–4948. PMID: 22050744
9. Baumgartner C, Graf M, Doppelbauer A, Serles W, Lindinger G, Olbrich A, et al. The Functional Organization of the Interictal Spike Complex in Benign Rolandic Epilepsy. Epilepsia. 1996; 37: 1164–1174. doi: 10.1111/j.1528-1157.1996.tb00548.x PMID: 8956847
10. Zhang ZJ, Valiante TA, Carlen PL. Transition to seizure: from "macro"- to "micro"-mysteries. Epilepsy Res. 2011; 97: 290–299. doi: 10.1016/j.eplepsyres.2011.09.025 PMID: 22075227
11. Shen X, Papademetris X, Constable RT. Graph-theory based parcellation of functional subunits in the brain from resting-state fMRI data. NeuroImage. 2010; 50: 1027–1035. doi: 10.1016/j.neuroimage.2009.12.119 PMID: 20060479
12. Huberfeld G, Menendez de la Prida L, Pallud J, Cohen I, Le Van Quyen M, Adam C, et al. Glutamatergic pre-ictal discharges emerge at the transition to seizure in human epilepsy. Nat Neurosci. 2011; 14: 627–634. doi: 10.1038/nn.2790 PMID: 21460834
13. Stam CJ. Modern network science of neurological disorders. Nat Rev Neurosci. 2014; 15: 683–695. doi: 10.1038/nrn3801 PMID: 25186238
14. Netoff TI, Clewley R, Arno S, Keck T, White JA. Epilepsy in small-world networks. J Neurosci Off J Soc Neurosci. 2004; 24: 8075–8083. doi: 10.1523/JNEUROSCI.1509-04.2004
15. Ponten SC, Bartolomei F, Stam CJ. Small-world networks and epilepsy: Graph theoretical analysis of intracerebrally recorded mesial temporal lobe seizures. Clin Neurophysiol. 2007; 118: 918–927. doi: 10.1016/j.clinph.2006.12.002 PMID: 17314065
16. Wilke C, Worrell G, He B. Graph analysis of epileptogenic networks in human partial epilepsy. Epilepsia. 2011; 52: 84–93. doi: 10.1111/j.1528-1167.2010.02785.x PMID: 21126244

17. Kramer MA, Kolaczyk ED, Kirsch HE. Emergent network topology at seizure onset in humans. Epilepsy Res. 2008; 79: 173–186. doi: 10.1016/j.eplepsyres.2008.02.002 PMID: 18359200

18. Rubinov M, Sporns O. Complex network measures of brain connectivity: uses and interpretations. NeuroImage. 2010; 52: 1059–1069. doi: 10.1016/j.neuroimage.2009.10.003 PMID: 19819337

19. Bullmore E, Sporns O. Complex brain networks: graph theoretical analysis of structural and functional systems. Nat Rev Neurosci. 2009; 10: 186–198. doi: 10.1038/nrn2575 PMID: 19190637

20. Bassett DS, Bullmore E. Small-world brain networks. Neurosci Rev J Bringing Neurobiol Neurol Psychiatry. 2006; 12: 512–523. doi: 10.1177/1073858406293182

21. Sporns O, Zwi JD. The small world of the cerebral cortex. Neuroinformatics. 2004; 2: 145–162. doi: 10.1385/NI:2:2:145 PMID: 15319512

22. Zhang Z, Liao W, Chen H, Mantini D, Ding J-R, Xu Q, et al. Altered functional-structural coupling of large-scale brain networks in idiopathic generalized epilepsy. Brain J Neurol. 2011; 134: 2912–2928. doi: 10.1093/brain/awr223

23. Wang L, Zhu C, He Y, Zang Y, Cao Q, Zhang H, et al. Altered small-world brain functional networks in children with attention-deficit/hyperactivity disorder. Hum Brain Mapp. 2009; 30: 638–649. doi: 10.1002/hbm.20530 PMID: 18219621

24. Stam CJ, de Haan W, Daffertshofer A, Jones BF, Manshanden I, van Walsum AM van C, et al. Graph theoretical analysis of magnetoencephalographic functional connectivity in Alzheimer's disease. Brain. 2009; 132: 213–224. doi: 10.1093/brain/awn262 PMID: 18952674

25. Oostenveld R, Fries P, Maris E, Schoffelen J-M. FieldTrip: Open Source Software for Advanced Analysis of MEG, EEG, and Invasive Electrophysiological Data. Comput Intell Neurosci. 2010; 2011: e156869. doi: 10.1155/2011/156869

26. Lachaux J-P, Rodriguez E, Le Van Quyen M, Lutz A, Martinerie J, Varela FJ. Studying single-trials of phase synchronous activity in the brain. Int J Bifurc Chaos. 2000; 10: 2429–2439. doi: 10.1142/S0218127400001560

27. Mormann F, Lehnertz K, David P, Elger C E. Mean phase coherence as a measure for phase synchronization and its application to the EEG of epilepsy patients. Phys Nonlinear Phenom. 2000; 144: 358–369. doi: 10.1016/S0167-2789(00)00087-7

28. Bassett DS, Meyer-Lindenberg A, Achard S, Duke T, Bullmore E. Adaptive reconfiguration of fractal small-world human brain functional networks. Proc Natl Acad Sci. 2006; 103: 19518–19523. doi: 10.1073/pnas.0606005103 PMID: 17159150

29. Humphries MD, Gurney K. Network "Small-World-Ness": A Quantitative Method for Determining Canonical Network Equivalence. PLoS ONE. 2008; 3. doi: 10.1371/journal.pone.0002051

30. Quraan MA, McCormick C, Cohn M, Valiante TA, McAndrews MP. Altered Resting State Brain Dynamics in Temporal Lobe Epilepsy Can Be Observed in Spectral Power, Functional Connectivity and Graph Theory Metrics. PLoS ONE. 2013; 8: e68609. doi: 10.1371/journal.pone.0068609 PMID: 23922658

31. He H, Sui J, Yu Q, Turner JA, Ho B-C, Sponheim SR, et al. Altered Small-World Brain Networks in Schizophrenia Patients during Working Memory Performance. PLoS ONE. 2012; 7: e38195. doi: 10.1371/journal.pone.0038195 PMID: 22701611

32. Maris E, Oostenveld R. Nonparametric statistical testing of EEG- and MEG-data. J Neurosci Methods. 2007; 164: 177–190. doi: 10.1016/j.jneumeth.2007.03.024 PMID: 17517438

33. Liu T, Lin P, Chen Y, Wang J. Electroencephalogram synchronization analysis for attention deficit hyperactivity disorder children. Biomed Mater Eng. 2014; 24: 1035–1039. doi: 10.3233/BME-130901 PMID: 24211994

34. Doesburg SM, Ribary U, Herdman AT, Cheung T, Moiseev A, Weinberg H, et al. Altered Long-Range Phase Synchronization and Cortical Activation in Children Born Very Preterm. IFMBE Proc. 2010; 29: 250–253. doi: 10.1007/978-3-642-12197-5_57 PMID: 21331353

35. Pfurtscheller G, Stancák A Jr., Neuper C. Event-related synchronization (ERS) in the alpha band—an electrophysiological correlate of cortical idling: A review. Int J Psychophysiol. 1996; 24: 39–46. doi: 10.1016/S0167-8760(96)00066-9 PMID: 8978434

36. Douw L, de Groot M, van Dellen E, Heimans JJ, Ronner HE, Stam CJ, et al. "Functional connectivity" is a sensitive predictor of epilepsy diagnosis after the first seizure. PloS One. 2010; 5: e10839. doi: 10.1371/journal.pone.0010839 PMID: 20520774

37. Douw L, van Dellen E, de Groot M, Heimans JJ, Klein M, Stam CJ, et al. Epilepsy is related to theta band brain connectivity and network topology in brain tumor patients. BMC Neurosci. 2010; 11: 103. doi: 10.1186/1471-2202-11-103 PMID: 20731854

38. Stoffers D, Bosboom JLW, Deijen JB, Wolters EC, Stam CJ, Berendse HW. Increased cortico-cortical functional connectivity in early-stage Parkinson's disease: an MEG study. NeuroImage. 2008; 41: 212–222. doi: 10.1016/j.neuroimage.2008.02.027 PMID: 18395468

39. Stam CJ, Jones BF, Manshanden I, van Cappellen van Walsum AM, Montez T, Verbunt JPA, et al. Magnetoencephalographic evaluation of resting-state functional connectivity in Alzheimer's disease. NeuroImage. 2006; 32: 1335–1344. doi: 10.1016/j.neuroimage.2006.05.033 PMID: 16815039

40. Xiao F, Chen Q, Yu X, Tang Y, Luo C, Fang J, et al. Hemispheric lateralization of microstructural white matter abnormalities in children with active benign childhood epilepsy with centrotemporal spikes (BECTS): A preliminary DTI study. J Neurol Sci. 2014; 336: 171–179. doi: 10.1016/j.jns.2013.10.033 PMID: 24210075

41. Kanemura H, Hata S, Aoyagi K, Sugita K, Aihara M. Serial changes of prefrontal lobe growth in the patients with benign childhood epilepsy with centrotemporal spikes presenting with cognitive impairments/behavioral problems. Brain Dev. 2011; 33: 106–113. doi: 10.1016/j.braindev.2010.03.005 PMID: 20381984

42. Kwon S, Seo H-E, Hwang SK. Cognitive and other neuropsychological profiles in children with newly diagnosed benign rolandic epilepsy. Korean J Pediatr. 2012; 55: 383–387. doi: 10.3345/kjp.2012.55.10.383 PMID: 23133485

43. Danielsson J, Petermann F. Cognitive deficits in children with benign rolandic epilepsy of childhood or rolandic discharges: a study of children between 4 and 7 years of age with and without seizures compared with healthy controls. Epilepsy Behav EB. 2009; 16: 646–651. doi: 10.1016/j.yebeh.2009.08.012

44. Verrotti A, Filippini M, Matricardi S, Agostinelli MF, Gobbi G. Memory impairment and Benign Epilepsy with centrotemporal spike (BECTS): a growing suspicion. Brain Cogn. 2014; 84: 123–131. doi: 10.1016/j.bandc.2013.11.014 PMID: 24362071

45. Tan B, Kong X, Yang P, Jin Z, Li L. The Difference of Brain Functional Connectivity between Eyes-Closed and Eyes-Open Using Graph Theoretical Analysis. Comput Math Methods Med. 2013; 2013. doi: 10.1155/2013/976365

46. Cohen M. Auditory/verbal and visual/spatial memory in children with complex partial epilepsy of temporal lobe origin. Brain Cogn. 1992; 20: 315–326. doi: 10.1016/0278-2626(92)90024-G PMID: 1449761

47. Liu Y, Liang M, Zhou Y, He Y, Hao Y, Song M, et al. Disrupted small-world networks in schizophrenia. Brain. 2008; 131: 945–961. doi: 10.1093/brain/awn018 PMID: 18299296

48. Li W, Douglas Ward B, Liu X, Chen G, Jones JL, Antuono PG, et al. Disrupted small world topology and modular organisation of functional networks in late-life depression with and without amnestic mild cognitive impairment. J Neurol Neurosurg Psychiatry. 2014; doi: 10.1136/jnnp-2014-309180

49. Ponten SC, Douw L, Bartolomei F, Reijneveld JC, Stam CJ. Indications for network regularization during absence seizures: Weighted and unweighted graph theoretical analyses. Exp Neurol. 2009; 217: 197–204. doi: 10.1016/j.expneurol.2009.02.001 PMID: 19232346

50. Wu H, Li X, Guan X. Networking Property During Epileptic Seizure with Multi-channel EEG Recordings. In: Wang J, Yi Z, Zurada JM, Lu B-L, Yin H, editors. Advances in Neural Networks—ISNN 2006. Springer Berlin Heidelberg; 2006. pp. 573–578. Available: http://link.springer.com/chapter/10.1007/11760191_84

51. Simard D, Nadeau L, Kröger H. Fastest learning in small-world neural networks. Phys Lett A. 2005; 336: 8–15. doi: 10.1016/j.physleta.2004.12.078

52. Percha B, Dzakpasu R, Żochowski M, Parent J. Transition from local to global phase synchrony in small world neural network and its possible implications for epilepsy. Phys Rev E. 2005; 72: 031909. doi: 10.1103/PhysRevE.72.031909

53. Barkley GL, Baumgartner C. MEG and EEG in epilepsy. J Clin Neurophysiol Off Publ Am Electroencephalogr Soc. 2003; 20: 163–178.

54. Ioannides AA. Dynamic functional connectivity. Curr Opin Neurobiol. 2007; 17: 161–170. doi: 10.1016/j.conb.2007.03.008 PMID: 17379500

55. He B, Dai Y, Astolfi L, Babiloni F, Yuan H, Yang L. eConnectome: A MATLAB Toolbox for Mapping and Imaging of Brain Functional Connectivity. J Neurosci Methods. 2011; 195: 261–269. doi: 10.1016/j.jneumeth.2010.11.015 PMID: 21130115

56. Nolte G, Ziehe A, Nikulin VV, Schlögl A, Krämer N, Brismar T, et al. Robustly Estimating the Flow Direction of Information in Complex Physical Systems. Phys Rev Lett. 2008; 100: 234101. doi: 10.1103/PhysRevLett.100.234101 PMID: 18643502

57. Li W, Wu N, Hou W, Zhang J, Xu W, Wu G, et al. Lateralization of epileptic foci through causal analysis of scalp-EEG interictal spike activity. J Clin Neurophysiol Off Publ Am Electroencephalogr Soc. 2015; 32: 57–65.

58. Wilke C, Ding L, He B. Estimation of time-varying connectivity patterns through the use of an adaptive directed transfer function. IEEE Trans Biomed Eng. 2008; 55: 2557–2564. doi: 10.1109/TBME.2008.919885 PMID: 18990625

59. Wilke C, van Drongelen W, Kohrman M, He B. Neocortical seizure foci localization by means of a directed transfer function method. Epilepsia. 2010; 51: 564–572. doi: 10.1111/j.1528-1167.2009.02329.x PMID: 19817817

60. Stanley ML, Moussa MN, Paolini BM, Lyday RG, Burdette JH, Laurienti PJ. Defining nodes in complex brain networks. Front Comput Neurosci. 2013; 7: 169. doi: 10.3389/fncom.2013.00169 PMID: 24319426

61. Nunez PL, Srinivasan R, Westdorp AF, Wijesinghe RS, Tucker DM, Silberstein RB, et al. EEG coherency: I: statistics, reference electrode, volume conduction, Laplacians, cortical imaging, and interpretation at multiple scales. Electroencephalogr Clin Neurophysiol. 1997; 103: 499–515. doi: 10.1016/S0013-4694(97)00066-7 PMID: 9402881

62. Blinowska KJ. Review of the methods of determination of directed connectivity from multichannel data. Med Biol Eng Comput. 2011; 49: 521–529. doi: 10.1007/s11517-011-0739-x PMID: 21298355

63. Sohrabpour A, Lu Y, Kankirawatana P, Blount J, Kim H, He B. Effect of EEG electrode number on epileptic source localization in pediatric patients. Clin Neurophysiol Off J Int Fed Clin Neurophysiol. 2015; 126: 472–480. doi: 10.1016/j.clinph.2014.05.038

64. Hassan M, Dufor O, Merlet I, Berrou C, Wendling F. EEG source connectivity analysis: from dense array recordings to brain networks. PloS One. 2014; 9: e105041. doi: 10.1371/journal.pone.0105041 PMID: 25115932